Supplemental Document

OPTICA

Line lasing in a two-dimensional lattice of orbital photonic resonators: supplement

TONY MATHEW BLESSAN,[1] BASTIAN REAL,[1] MARIJANA MILICEVIC,[2] ISABELLE SAGNES,[2] ARISTIDE LEMAÎTRE,[2] LUC LE GRATIET,[2] ABDELMOUNAIM HAROURI,[2] SYLVAIN RAVETS,[2] JACQUELINE BLOCH,[2] CLÉMENT HAINAUT,[1] AND ALBERTO AMO[1,*]

[1] *Univ. Lille, CNRS, UMR 8523—PhLAM—Physique des Lasers Atomes et Molécules, F-59000 Lille, France*
[2] *Université Paris-Saclay, CNRS, Centre de Nanosciences et de Nanotechnologies, 91120 Palaiseau, France*
[*] *alberto.amo-garcia@univ-lille.fr*

Supplement DOI: https://doi.org/10.6084/m9.figshare.32791641

Parent Article DOI: https://doi.org/10.1364/OPTICA.588387

Line lasing in a two-dimensional lattice of orbital photonic resonators: Supplemental Material

This document provides additional information and data.

1. EXPERIMENTAL SCHEME

Figure S1 illustrates the experimental setup. The sample consists of a Lieb *sp* lattice placed inside a vacuum within a closed cycle helium cryostat and maintained at a temperature of 4 K, as recorded at the sample holder. A narrow linewidth (<10MHz) single-mode Ti:Sapphire laser serves as the excitation source (wavelength 820nm). The beam is delivered through a single mode polarization maintaining optical fiber to ensure a high quality Gaussian spatial profile. After exiting the fiber, the beam power is regulated using a combination of a half-wave plate ($\lambda/2$) and a polarizing beam splitter (PBS), which together serve as a tunable power control unit. To generate two different excitation spots we divide the excitation beam in using a beamsplitter. Each arm is equipped with a cylindrical lens (focal length $f = 700$ mm) to create elongated Gaussian spots independently in each arm. The beams are then recombined at a PBS, forming the final excitation profile. A portion of the beam is diverted by a beam splitter (BS) for power monitoring, while the rest is directed toward the sample for excitation.

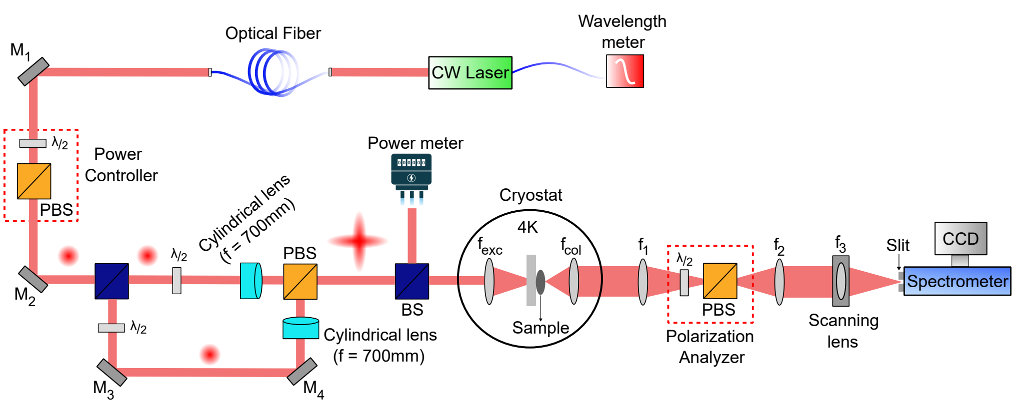

Fig. S1. Scheme of the experimental setup illustrating the excitation of the Lieb *sp* lattice and real space imaging of polariton photoluminescence (PL). Abbreviations: $\frac{\lambda}{2}$ - half-wave retarder, PBS - polarized beam splitter, BS - beam splitter. Lenses: f_{exc}, f_{col} = 8 mm, f_1 = 300 mm, f_2 = 150 mm and f_3 = 500 mm.

The measurements are carried out in a transmission geometry: the excitation beams enter the sample through the epitaxial side, propagate through the substrate, and exit via a 3mm slit in the sample holder before reaching the collection optics. Both excitation and detection optics employ aspheric lenses (f_{exc}, f_{col}) with a numerical aperture of 0.5. It is worth noting that the GaAs substrate exhibits negligible absorption at the operating wavelength allowing efficient light transmission. The photoluminescence emitted from the sample is first magnified using a telescope composed of two lenses with focal lengths f_1 and f_2. Following this, the beam passes through a polarization analysis setup consisting of a half-wave plate ($\lambda/2$) and a polarizing beam splitter (PBS). The transmitted light is then collected by a scanning objective lens (f_3) and directed either to a CCD camera for imaging or to a spectrometer for spectral analysis. For Fourier space imaging, an additional lens is inserted between the telescope and the scanning lens.

2. LINE LASING IN A 10×10 LATTICE

In the main manuscript, the experimental results were presented for a 4×4 lattice configuration. To demonstrate that the observed line lasing behavior and polarization locking phenomena are

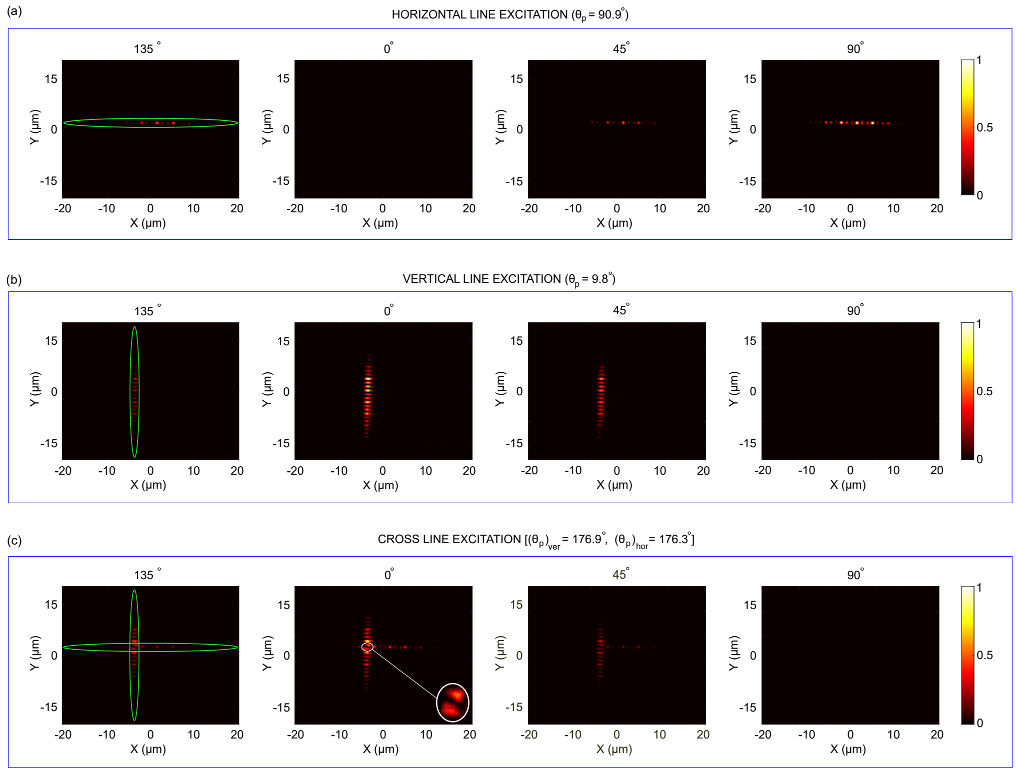

Fig. S2. Real space photoluminescence (PL) images analyzed at four output polarization angles: 135°, 0°, 45°, and 90°, using a polarization analyzer consisting of a half-wave plate and linear polarizer. 0° corresponds to horizontal polarization. (a) PL from the horizontal line with horizontal spot excitation at P = 35mW. (b) PL from the vertical line with vertical spot excitation at P = 35mW. (c) PL under cross pumping excitation with a total power of 71mW. All images are extracted at a fixed energy slice (top *sp* band).

not specific to the system size, here we present measurements performed on a larger 10×10 lattice etched in the same microcavity wafer.

Real space imaging of the polariton photoluminescence was performed at the top of the *sp* band under a horizontally elongated excitation spot. All panels in Fig. S2(a) were taken above the lasing threshold, with a pump power of 35 mW. The emission was recorded for four linear output polarization angles: 135°, 0°, 45°, and 90°, corresponding to distinct analyzer orientations. In Fig. S2(b), a similar set of measurements was carried out using a vertically elongated excitation spot, also pumped above threshold at 35 mW. Real space images were recorded under the same set of output polarization angles (135°, 0°, 45°, and 90°). In the cross-pump excitation configuration as shown in Fig. S2(c), real space emission was again recorded under the four linear analyzer angles at a combined total power of 71 mW.

To extract the orientation of linear polarization from the measured photoluminescence for above three cases, intensities obtained by integrating the PL signal along a fixed energy (top of *sp* band) is calculated at four linear polarization analyzer angles: 135°, 0°, 45°, and 90° respectively. The Stokes parameters S_0, S_1, and S_2 were calculated using the following relations:

$$S_0 = I_{0^\circ} + I_{90^\circ} \tag{S1}$$

$$S_1 = I_{0^\circ} - I_{90^\circ} \tag{S2}$$

$$S_2 = I_{45^\circ} - I_{135^\circ} \tag{S3}$$

$$S_3 = 0 \quad \text{(assuming negligible circular polarization)} \tag{S4}$$

The angle of linear polarization is calculated using:

$$\theta_p = \frac{1}{2} \tan^{-1} \left(\frac{S_2}{S_1} \right) \tag{S5}$$

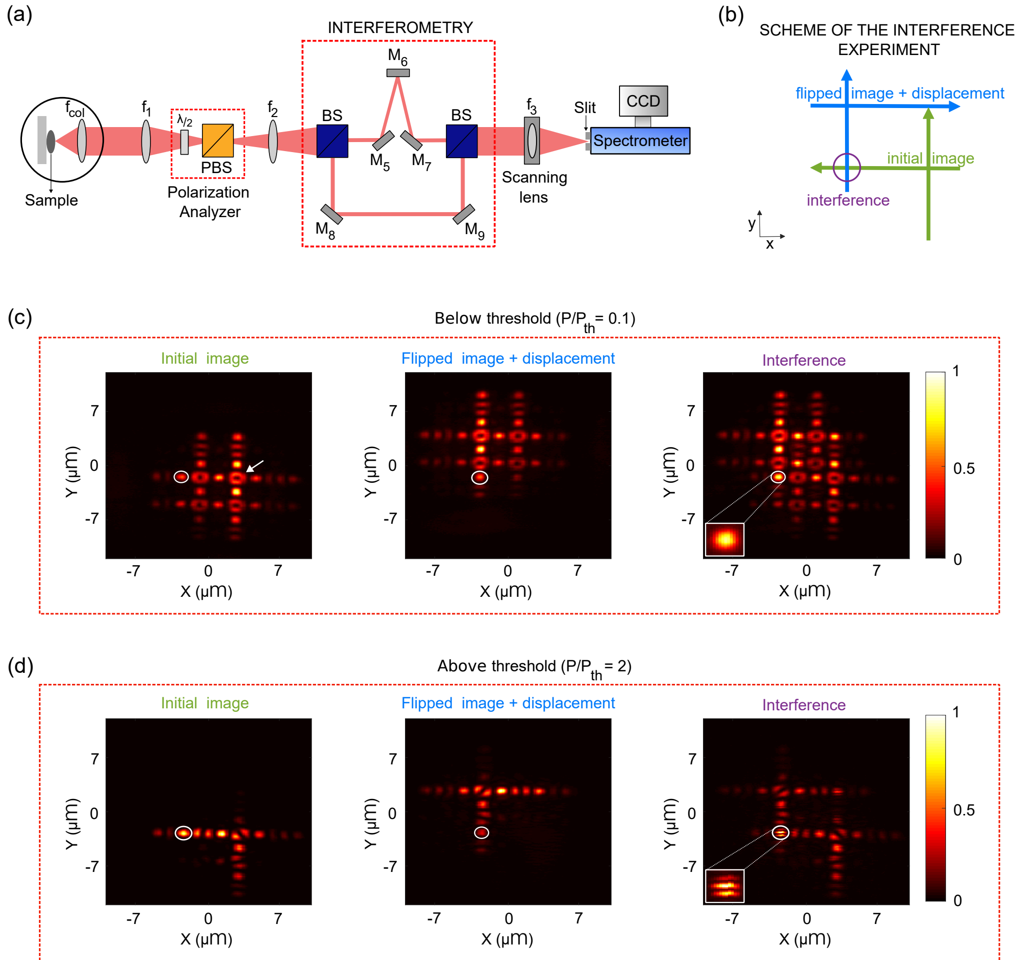

Fig. S3. (a) Schematic of the experimental setup for the interferometry. (b) Illustration of the interference procedure: the initial image is flipped and spatially displaced then recombined to produce the interference pattern. (c) Interferogram recorded below threshold power, where no interference is observed (shown as an inset). (d) Interferogram recorded above the threshold power, revealing clear interference fringes (shown as an inset).

The computed angle θ_p gives the polarization of the line lasing mode. For horizontal excitation, $\theta_p = 90.9^\circ$ (vertical polarization), while for vertical excitation, $\theta_p = 9.8^\circ$(horizontal polarization). Under cross-pump conditions, the vertical line yields $(\theta_p)_{\text{ver}} = 176.9^\circ$ (horizontally polarized) and the horizontal line gives $(\theta_p)_{\text{hor}} = 176.3^\circ$ (horizontally polarized). These results confirm that the two line modes are both phase (as shown in the inset of Fig. S2(c)) and polarization locked, consistent with the behavior observed in the 4×4 lattice.

Note that the power arrangement between the two pump spots shown in the main paper with a 4×4 lattice resulted in vertical polarization locking. In the experiments displayed in Fig. S2 for a 10×10 lattice the two spots have slightly different powers ($P_{horarm} = 38$ mW and $P_{verarm} = 33$ mW) such that the local blueshifts result in an energy degeneracy of modes with horizontal polarization.

3. INTERFERENCE EXPERIMENT

To confirm the phase locking of the two orthogonal line modes, an interferometric measurement was performed. Fig. S3(a) shows the interferometer configuration using three mirrors, with mirror M_6 mounted on a kinematic stage for fine adjustment. This allows precise control of the optical path length to achieve near zero delay between the two arms, which is essential for observing interference and verifying phase coherence between the modes.

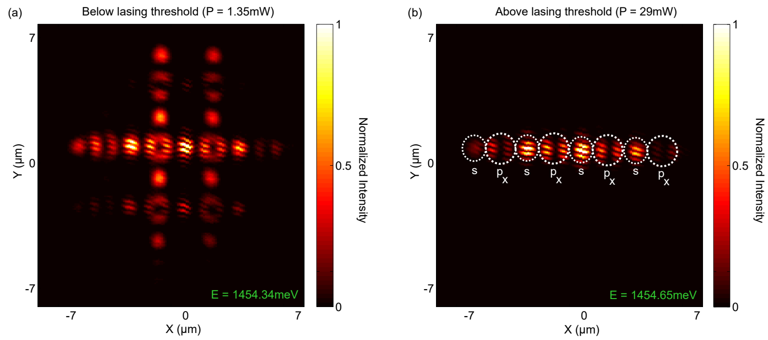

Fig. S4. Interference of the emission with an horizontal mirror image of itself at the energy of the top of the *sp* band at (a) low power below lasing threshold and, (b) high power above lasing threshold.

Figure S3(b) illustrates the schematic of the interference process. One arm of the interferometer captures the direct image of the emission, while the other arm produces a spatially displaced and mirror-flipped version of the same image. This configuration allows the two images to overlap and interfere.

Figure S3(c) - left panel- shows the initial image below threshold. Emission is spread over several lines in the lattice. At the crossing site of the two pump spots (see arrow), we observe a ring like emission. This ring pattern is characteristic of the random phase between the p_x and p_y orbitals in the spontaneous emission regime below threshold. The white circles in the left and central images of Fig. S3(c) highlight the spatial regions where the *s*-orbital modes from the two orthogonal lines are made to interfere in the right panel. The absence of interference fringes witnesses the absence of phase locking in the spontaneous emission regime at $P/P_{th} = 0.1$. Above threshold ($P/P_{th} = 2$), Fig. S3(d) shows the emergence of interference fringes, clearly visible in the inset of the right panel, indicating phase locking.

4. SPATIAL COHERENCE OF THE LINE LASER

Using the experimental setup described in the previous section we study the spatial coherence of an individual line laser in the conditions of Fig. 3. Figure S4 displays the interference of the emission at the energy of the top of *sp* band with its horizontal mirror image without any vertical shift and at optical contact (zero time delay). At x=0, the small pillar in the center of the line interferes with itself. At each value of x, the emission interferes with the emission at -x. Above the lasing threshold, Fig. S4(b), very high visibility of fringes can be observed all along the line, indicating a high spatial coherence. Below threshold, Fig. S4(b), the central horizontal line still displays interference fringes of lower visibility at the sides. The origin of the observed spatial coherence below threshold is the the finite size of the lattice: it slightly splits different modes which present long enough spontaneous coherence to give rise to visible fringes in this interferometric experiment.

5. POLARIZATION RESOLVED EMISSION

In this section we provide additional experimental details on the polarization resolved emission for the crossed lines excitation. We focus on the conditions described in the main text for the crossed lines excitation of a 4×4 lattice reported in Fig. 5.

Figures S5(a) and (b) display the porlarization resolved emission integrated spatially over each of excited lines (vertical line in (a), horizontal line in (b)) at the energy of the top of the *sp* bands. The horizontal axis corresponds to the total excitation power (sum of the power of the two spots). Above threshold, the degree of linear vertical polarization is high for both lines.

In the main text of Fig. 5(c) analysis of blueshift was done at $P/P_{th} = 1.2$. As an additional proof, Fig. S5(c) shows the energy spectra of the emission along the vertical and horizontal lasing lines with the analyzer in the vertical linear polarization position, which corresponds to the polarization of the laser emission, for an excitation power well above threshold ($P/P_{th} = 1.6$). The laser emission energy in this polarization for the modes at the top of the *sp* bands is identical up to our spectral resolution (dashed line). Figure S5(d) shows the energy spectra of the emission

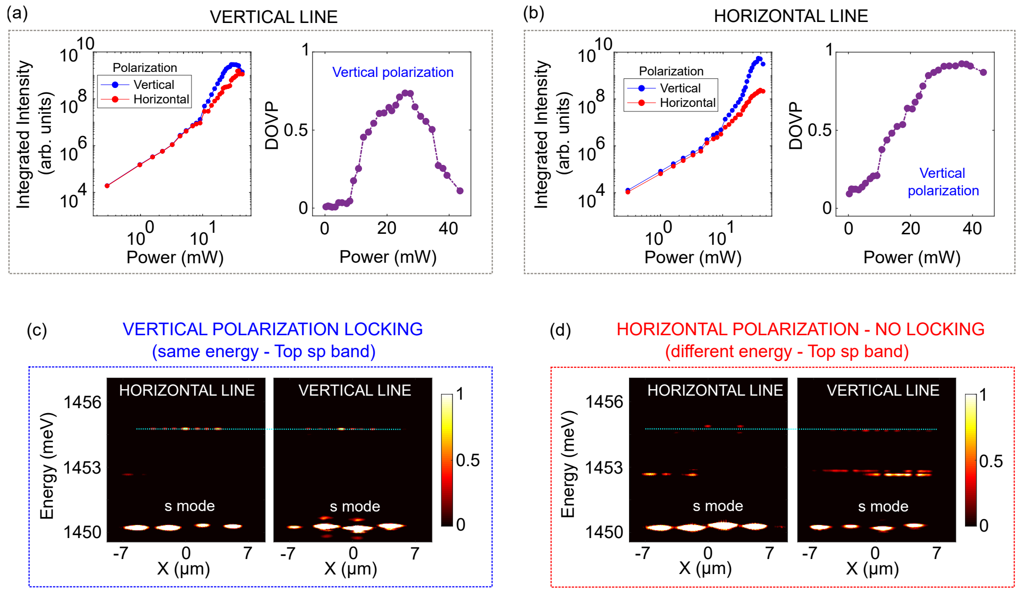

Fig. S5. (a) Integrated intensity of the upper *sp* mode along the vertical line for a cross pump configuration. The intensity is resolved in linear polarization and the degree of vertical polarization (DOVP) is computed from the integrated intensity. (b) Same as (a) for the horizontal line in the cross pumping configuration. (c) Measured spectrum of the vertically polarized emission along the vertical and horizontal line. The dashes line is a reference to show the vertically polarized *sp* modes in both lines is are energetically aligned. (d) Measured spectrum of the horizontally polarized emission. It displays an energy mismatch between the horizontally polarized top *sp* modes in the two lines.

with opposite polarization (horizontal), for the two lasing lines. Emission from the top of the *sp* bands is weaker but still visible. However, it does not happen at the energy of the vertical polarization emission of the lasing mode in Fig. S5(c). Each line of the lattice emits horizontally polarized light at the top of the *sp* band at different energies. This polarization behavior is displayed in Fig. 5(d) of the main text. It shows that different blueshifts on each line are required for polarization alignment and locking of the lasing mode.

6. SIMULATION OF POLARIZATION LOCKING IN THE CROSS LINES LASER

The simulation of lasing in the cross configuration including the polarization degree of freedom, the local blueshifts and the confinement induced splittings is not an easy task and goes beyond the scope of this work. Nevertheless, we now present a phenomenological simulation that studies the effect of the energy alignment of polarizations in the two pumped lines in the lasing regime. To do so, we start from the model in Eqs. (4)-(6) of the main text. We double the Hilbert space to include the polarization degree of freedom in the horizontal-vertical basis for each orbital at each site. The two polarization modes are fed from the same reservoir, which is fed by a pump in cross geometry. Our goal is to simulate the lasing regime above threshold. In this situation, in the experiment, the local pump reservoirs induce a blueshift that detaches the two lines from the rest of the lattice resulting in a splitting of the linear polarizations parallel and perpendicular to each line. We introduce this splitting by hand, with a value of 0.12 meV, as measured in the experiment (see Fig. 3(c)).

If the blueshift of the two lines is the same, then the vertical polarization mode of the horizontal line matches the horizontal polarization mode of the vertical line and each line lases in a different polarization without any phase locking (Fig. S6(a)). If we now shift the local potential of the sites of the horizontal line by 0.12 meV with respect to the vertical line, the vertically polarized modes of the two lines match in energy. In this situation, the simulation shows cross lasing in both lines in vertical polarization and phase locked (Fig. S6(b)). This precisely the situation of the experiment shown in Fig. 5 of the main text. If we now invert the local potentials such that the vertical line sites are 0.12 meV above the horizontal line, then the horizontally polarized

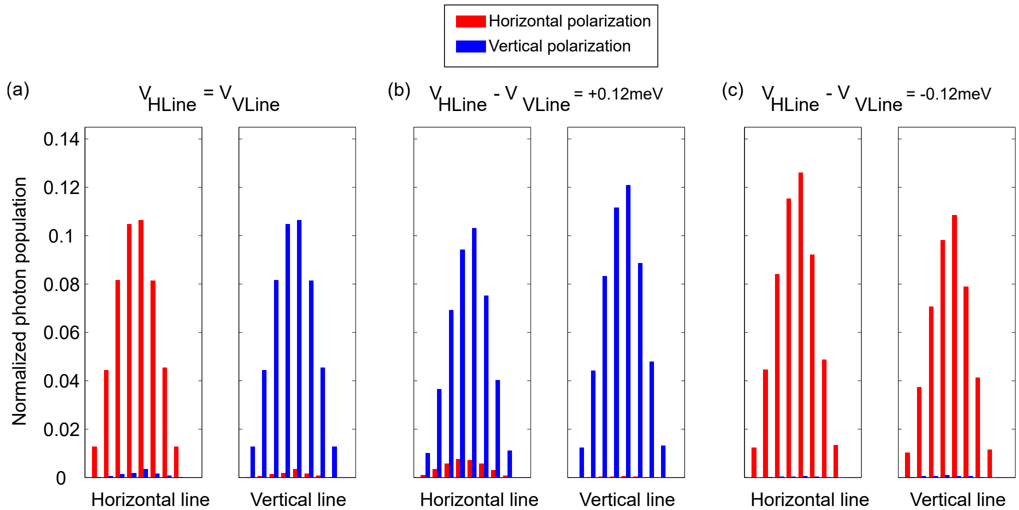

Fig. S6. Simulated lasing emission above threshold resolved in polarization in three different configurations under cross line pumping as in the experiments displayed Fig. 5 of the main text. In the simulations, the Hilbert space in Eqs. (4)-(6) has been doubled to take into account the polarization degree of freedom in each orbital. An horizontal-vertical polarization splitting of 0.12 meV has been set at the horizontal pumped line, and a splitting of -0.12meV at the vertical pumped line. (a) Lasing emission resolved in horizontal and vertical polarization in each line in the described model. The bars display the emitted intensity at each site of the line. Each line lases in a different polarization. (b) Same as (a) when a local onsite potential of 0.12 meV is set on all sites of the horizontal line. In this situation the vertically polarized emission of the two lines is aligned and the system lases phase locked in vertical polarization. (c) Same as (a) when a local onsite when a local onsite potential of 0.12 meV is set on all sites of the vertical line. In this situation the horizontally polarized emission of the two lines is aligned and the system lases phase locked in horizontal polarization.

modes are aligned in energy and the simulation produces horizontally polarized lasing with phase locking between lines (Fig. S6(c)). This is the experimental situation displayed in Fig. S2.